# Synthesis of Carboxylate Cp*Zr(IV) Species: Towards the Formation of Novel Metallocavitands

*Maxime Daigle,*[a,b,c] *Wenhua Bi,*[a] *Marc-André Légaré,*[a,c] *Jean-François Morin** [a,b] *and Frédéric-Georges Fontaine** [a,c]

[a] Département de Chimie, Université Laval, 1045 Avenue de la Médecine, Québec (Québec), Canada, G1V 0A6

[b] Centre de Recherche sur les Matériaux Avancés (CERMA), Université Laval

[c] Centre de Catalyse et Chimie Verte (C3V), Université Laval

Emails : frederic.fontaine@chm.ulaval.ca and jean-francois.morin@chm.ulaval.ca

***This is the peer reviewed version of the following article: [Synthesis of Carboxylate Cp*Zr(IV) Species: Towards the Formation of Novel Metallocavitands, Inorg. Chem. 2015, 54, 5547−5555], which has been published in final form at [10.1021/acs.inorgchem.5b00634].***

**Abstract**

In the intent of generating metallocavitands isostructural to species $[(CpZr)_3(\mu^3\text{-}O)(\mu^2\text{-}OH)_3(\kappa_{O,O,}\mu^2\text{-}O_2C(R))_3]^+$, the reaction of $Cp^*_2ZrCl_2$ and $Cp^*ZrCl_3$ with phenylcarboxylic acids was carried out. Depending on the reaction conditions, five new complexes were obtained, which consisted of $Cp^*_2ZrCl(\kappa^2\text{-}OOCPh)$ (**1**), $(Cp^*ZrCl(\kappa^2\text{-}OOCPh))_2(\mu\text{-}\kappa^2\text{-}OOCPh)_2$ (**2**), $[(Cp^*Zr(\kappa^2\text{-}OOCPh))_2(\mu\text{-}\kappa^2\text{-}OOCPh)_2(\mu^2\text{-}OH)_2]\bullet Et_2O$ (**3•Et₂O**), $[[Cp^*ZrCl_2](\mu\text{-}Cl)(\mu\text{-}OH)(\mu\text{-}O_2CC_6H_5)[Cp^*Zr]]_2(\mu\text{-}O_2CC_6H_5)_2$ (**4**) and $[Cp^*ZrCl_4][(Cp^*Zr)_3(\kappa_2\text{-}OOC(C_6H_4Br)_3(\mu_3\text{-}O)(\mu_2\text{-}Cl)_2(\mu_2\text{-}O\mathit{H})]$ [**Cp*ZrCl₄**][**5**]. The structural characterization of the five complexes was carried out. Species **3•Et₂O** exhibits host-guest properties where the diethyl ether molecule is included in a cavity formed by two carboxylate moieties. The secondary interactions between the cavity and the diethyl ether molecule affect the structural parameters of the complex, as demonstrated be the comparison of the DFT models for **3** and **3•Et₂O**. Species **5** was shown to be isostructural to the $[(CpZr)_3(\mu^3\text{-}O)(\mu^2\text{-}OH)_3(\kappa_{O,O,}\mu^2\text{-}O_2C(R))_3]^+$ metallocavitands.

## Introduction

Since the discovery of supramolecular assemblies in biological systems, there has been an ongoing interest in the design of supramolecular devices for various purposes, notably for molecular recognition[1] and catalysis.[2] Although several supramolecular architectures have been explored, cavitands are a class of molecules of particular interest. These species act as molecular cavities that can host an array of guest molecules according to shape and/or specific weak interactions, such as hydrogen bonding and π-π interactions. The most common cavitands are based on organic frameworks [3] and include notably calixarenes, [4] cucurbiturils, [5] cyclotriveratrylenes, [6] cyclodextrines, [7] and resorci-*n*-arenes. [8] Although these molecules are robust and quite versatile, the tailoring of organic cavitands often requires multistep syntheses that can be tedious and low yielding. One way to obtain cavitands while reducing the synthetic work is using self-assembly processes between organic ligands and metal precursors to generate metallocavitands.[9] In addition to the ease of synthesis, the presence of metal sites within the cavitand can bring additional properties, such as inducing catalytic activity, facilitating electronic communication or allowing molecular sensing.

In the past few years, our research group has been interested in the synthesis and properties of conical metallocavitands possessing $C_3$-symettry. In a first iteration, the addition of arylboronic acids to Cp*$TaMe_4$ afforded tantalum(V) boronate half-sandwich metallocavitands where the trimetallic core is comprised of one $\mu^3$-OH, one $\mu^2$-OH, two $\mu^2$-O, and three $\mu^2$-$O_2$BR bridges (Scheme 1A).[10] By modifying the nature of the arylboronic acid used in the synthesis, it was possible to obtain extended cavities that could host Lewis bases, such as acetone and THF.[10c]

The guests were shown to be stabilized by hydrogen bonding and by electrostatic interactions, a consequence of the electrophilicity of the boron atoms. [10b] However, these species did show signs of hydrolysis under basic conditions by cleavage of a B-C bond of the boronate moiety. In order to increase the stability of the metallocavitands, the synthesis of zirconium(IV) carboxylate half-sandwich metallocavitands was carried out.[11] Following reported procedures,[12] the addition of carboxylate ligands to $Cp_2ZrCl_2$ afforded trimetallic clusters having similar structural properties than the tantalum metallocavitands, but with a metallic core stabilized by a $\mu^3$-O, three $\mu^2$-OH and three $\mu^2$-$O_2CR$ bridges (Scheme 1B). We demonstrated that the incorporation of nitrogen-containing carboxylate moieties, such as carbazole and diphenylamine, in these zirconium metallocavitands could increase the blue luminescence properties of the pristine organic chromophores,[11b] and that the incorporation of exTTF units on the carboxylate ligands could generate hosts for fullerenes.[11a] However, in the latter complexes, the cyclopentadienyl ligand (Cp) was used rather than the pentamethylcyclopentadienyl (Cp*) used in the tantalum clusters. Since it is known that modifying a Cp for Cp* can increase the stability and solubility of the resulting complexes, which are important prerogatives for the preparation of supramolecular devices, we explored the synthesis of Cp*-Zr(IV) carboxylate metallocavitands. Although the chemistry of Zr(IV) cyclopentadienyl analogues bearing carboxylate ligands is abundant, the number of carboxylate complexes with the more electron-donating Cp* analogues remains quite limited, [13-14] and is usually resulting from the $CO_2$ insertion into Zr-R bonds.[14] Herein we report the generation of polymetallic carboxylate zirconium species by the addition of carboxylic acids to Zr(IV) pentamethylcyclopentadienyl precursors and the formation of mixed oxo-chlorido clusters, having in one instance a pseudo $C_3$ symmetry. One of these species, compound

$[(Cp^*Zr(\kappa^2\text{-}OOCPh))_2(\mu\text{-}\kappa^2\text{-}OOCPh)_2(\mu^2\text{-}OH)_2]$ (**3**) presents interesting host-guest interactions with $Et_2O$ at the solid state.

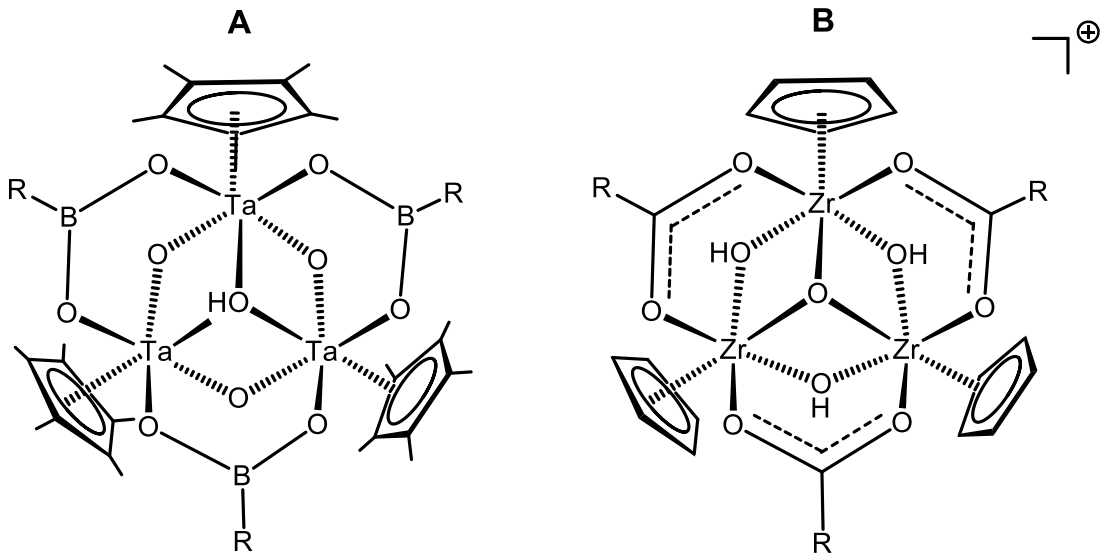


**Scheme 1.** A) Cp*Ta(V) boronate and B) CpZr(IV) carboxylate clusters

## Results and discussion

### Synthesis of zirconium(IV) metallocavitands

In a first attempt to generate Cp*Zr(IV) carboxylate metallocavitands, a similar approach to the synthesis of CpZr(IV) carboxylate species was carried out. It was shown that the addition of carboxylic acids to a solution of $Cp_2ZrCl_2$ in a dichloromethane and water solution at pH 7 could afford species of general structure $[(CpZr)_3(\kappa_2,O',O''CR)_3(\mu_3\text{-}O)(\mu_2\text{-}OH)_3].HCl$.[15] As one might expect, the addition of benzoic acid to $Cp^*_2ZrCl_2$ did not afford the trimetallic cluster but rather species $Cp^*_2ZrCl(\kappa^2\text{-}OOCPh)$ (**1**), as illustrated on Scheme 2. Using $^1H$ NMR spectroscopy, it was possible to observe the resonance for the aromatic protons at $\delta$ = 8.10, 7.56 and 7.44, while the Cp* resonance integrating for 30 protons relative to the resonances of the aryl ring was observed at 1.88 ppm. The same compound was obtained when varying the pH of the solution

from 7 to 10, but at pH 12, an insoluble white powder was obtained. Contrarily to the chemistry observed with the cyclopentadienyl analogues where species $Cp_2Zr(\kappa^2\text{-}OOCPh)_2$ is also present when $Cp_2ZrCl(\kappa^2\text{-}OOCPh)$ is generated under acidic conditions,[15] the bis(carboxylate) species $Cp^*_2Zr(\kappa^2\text{-}OOCPh)_2$ was not observed under our experimental conditions. It is likely that the steric hindrance as well as the electron donating capability of the Cp* makes difficult the formation of 20-electron species $Cp^*_2Zr(\kappa^2\text{-}OOCPh)_2$.

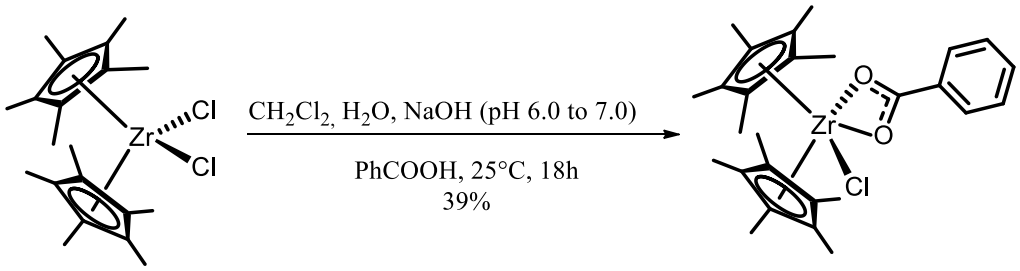


**Scheme 2.** Synthesis of complex $Cp^*_2ZrCl(\kappa^2\text{-}OOCPh)$ (**1**).

It was possible to obtain X-ray quality crystals of compound **1** by recrystallizing out of $CH_2Cl_2$. According to the X-ray diffraction analysis results, **1** crystalized in the central symmetric space group of $\boldsymbol{P}2_1/c$. The central Zr atom is coordinated by two Cp* ligands, one chloride, and two O atoms from the chelating carboxylate group. As shown in Figure 1, the structure shows a distorted trigonal bipyramidal configuration with a five-coordination number at the central Zr atom. The Zr-O bond lengths are of 2.257(4) and 2.300(4) Å, which are comparable to those in the structure of $[Cp^*_2Zr(\kappa^1\textit{O}\text{-}O_2C(C_6H_4\text{-}4\text{-}SH)(\kappa^2\text{-}O_2C(C_6H_4\text{-}4\text{-}SH)]$ (2.2722(16) and 2.3043(17) Å).[13b] The distances between the Zr atom and the centres of two Cp* planes are of 2.259(2) and 2.316(6) Å. The dihedral angle between the two Cp* rings is 42.3(2)°, with the plane of the chelated carboxylate group ($Zr_1\text{-}O_1\text{-}C_{31}\text{-}O_2$) being located in the middle of this angle as represented by the dihedral angles between the Cp* planes and the carboxylate plane of 21.9(2) and 20.4(2)°, respectively. It is noteworthy to mention that the chloride ligand is located within

the Zr-carboxylate plane, as illustrated in Figure 1. By looking at the packing model, it is possible to observe that the molecules of **1** are packed together into sheets in the ***b-c*** plane with the sheets further arranged together along the ***a*** axis to form a 3D framework, as shown in Figures S8-S9. No strong π-π interaction was found in the structure.

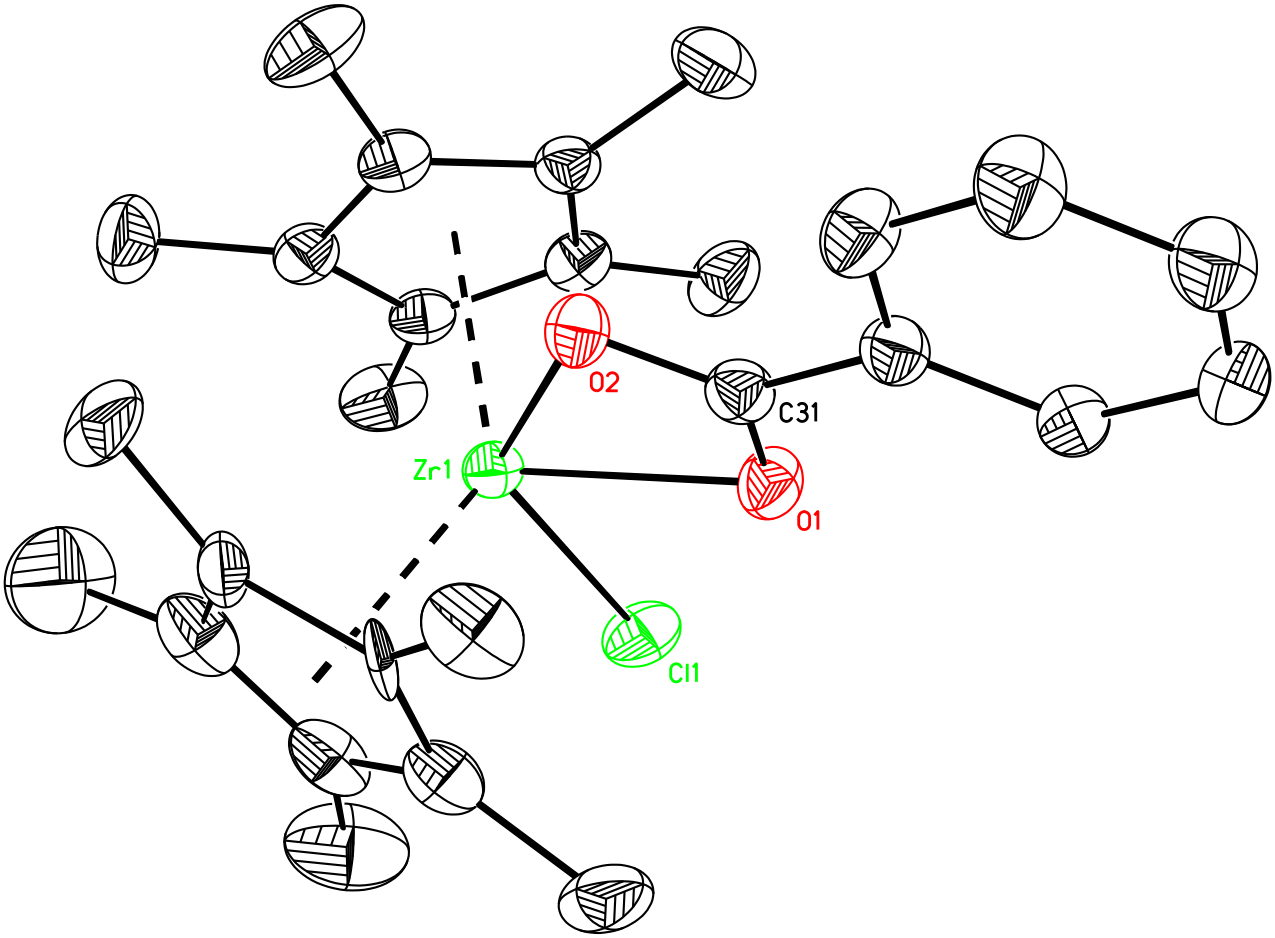


**Figure 1.** ORTEP drawing of **1** at 50% probability. H atoms are omitted for clarity. Only one orientation of the disordered Cp* group was plotted.

Species $Cp^*ZrCl_3$, that was synthesized using a protocol developed by Teuben and co-workers,[16] was used as a precursor in an attempt to generate the desired metallocavitands.

$Cp^*ZrCl_3$ was added to two equivalents of benzoic acid and one equivalent of water in THF at -78 °C and then agitated for 18 hours at ambient temperature until a colorless solution was formed. Quite interestingly, removal of the volatiles afforded a white powder that turned purple under prolonged exposure to reduce pressure. When the solid obtained was dissolved back in diethyl ether, a colorless solution was obtained once more. Slow evaporation of the ether solution afforded a mixture of two crystalline materials, $(Cp^*ZrCl(\kappa^2\text{-}OOCPh))_2(\mu\text{-}\kappa^2\text{-}OOCPh)_2$ (**2**) and $[(Cp^*Zr(\kappa^2\text{-}OOCPh))_2(\mu\text{-}\kappa^2\text{-}OOCPh)_2(\mu^2\text{-}OH)_2]\bullet Et_2O$ (**3•Et₂O**) (Scheme 3). Whereas only few crystals of **2** were obtained which prevented solution characterization, it was possible to observe that species **3•Et₂O** exhibits lower symmetry in solution, presumably a consequence of the dissociation of the ether molecule and the possible coexistence of more than one species in solution, notably by the presence of several resonances for the phenyl groups between δ 6.96 and 8.17 and by the presence of two Cp* resonances, each integrating for 15H at 2.03 and 2.06 ppm.

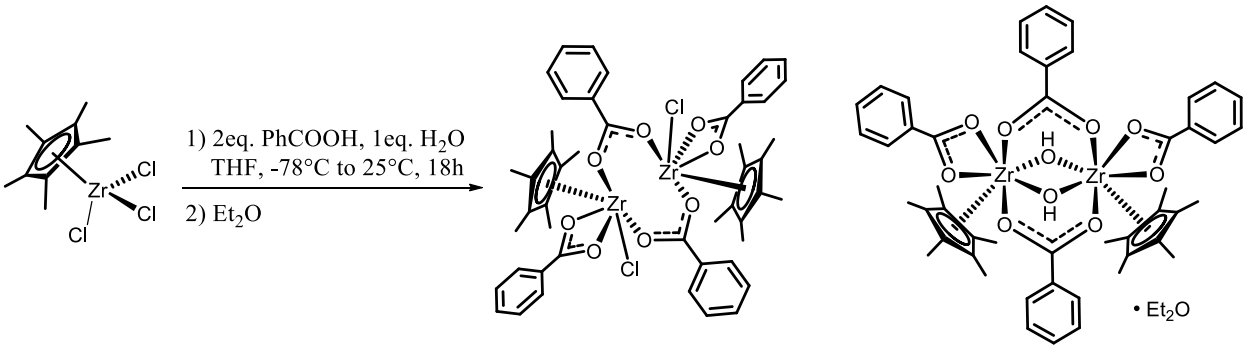


**2** **3**

**Scheme 3 :** Synthesis of complexes $(Cp^*ZrCl(\kappa^2\text{-}OOCPh))_2(\mu\text{-}\kappa^2\text{-}OOCPh)_2$ (**2**) and $[(Cp^*Zr(\kappa^2\text{-}OOCPh))_2(\mu\text{-}\kappa^2\text{-}OOCPh)_2(\mu^2\text{-}OH)_2]\bullet Et_2O$ (**3•Et₂O**).

Compound **2** crystalized in the non-classical central symmetric space group ***P***$2_1/n$. The central Zr atom is coordinated by one Cp* ligand, one chloride, and two oxygen atoms from one chelating

carboxylate group. Two adjacent Zr centres are linked together by two bridging carboxylate groups to form a charge-balanced dimer. Only half of the dimer is located in the asymmetric unit cell, the other part being generated by the inversion operation. As shown in the representation in Figure 2, each metal centre of the dimeric structure consists in a six-coordinated zirconium atom in a heavily distorted octahedron. The Zr-$O_3$ and Zr-$O_4$ bond lengths for the chelated carboxylate ligand are of 2.204(4) and 2.297(4) Å, respectively, whereas the Zr-$O_1$ and Zr-$O_2$ distances for the bridging ligands are significantly shorter at 2.166(3) and 2.079(3) Å, respectively. The Zr-O distances of the chelating ligand are slightly shorter that those observed in the structure of [Cp*$_2$Zr($\kappa^1$*O*-$O_2C(C_6H_4$-4-SH)($\kappa^2$-$O_2C(C_6H_4$-4-SH)] [13b] (2.2722(16) to 2.3043(17) Å) and in **1** (2.257(4) and 2.300(4) Å). The Zr-Cl distance of 2.4658(15) Å is slightly longer than those in the structure of (Cp)(Cp*)$ZrCl_2$ (2.4421(9) Å)[17] but slightly longer than in **1** (2.4954(17) Å). Replacing one bulky Cp* by a benzoate moiety greatly reduces the steric environment around the metal center, which can be observed by the short Zr-Cp*$_{centroid}$ distance of 2.211 Å, which is shorter than in **1** (2.259(2) and 2.316(6) Å). The strength of the Zr-Cp* interaction is further exemplified by the three O and the Cl atoms being pushed towards the other vertex of the octahedron (Zr-$O_4$), as shown by the cissoids angles ($O_2$-$Zr_1$-$O_4$, $O_1$-$Zr_1$-$O_4$, $O_3$-$Zr_1$-$O_4$, $O_4$-$Zr_1$-$Cl_1$) being lower than 90°. The bridging carboxylate group is twisted from the plane of the aromatic ring with a dihedral angle of 22.3(4)°. The distance between two Zr centres in the dimer is 5.2146(13) Å. The dimers of **2** are packed together into chains along the ***a*** axis (Figure S11) with the chains further aligned together in the ***a-c*** plane to form a 3D framework, as shown in Figure S12.

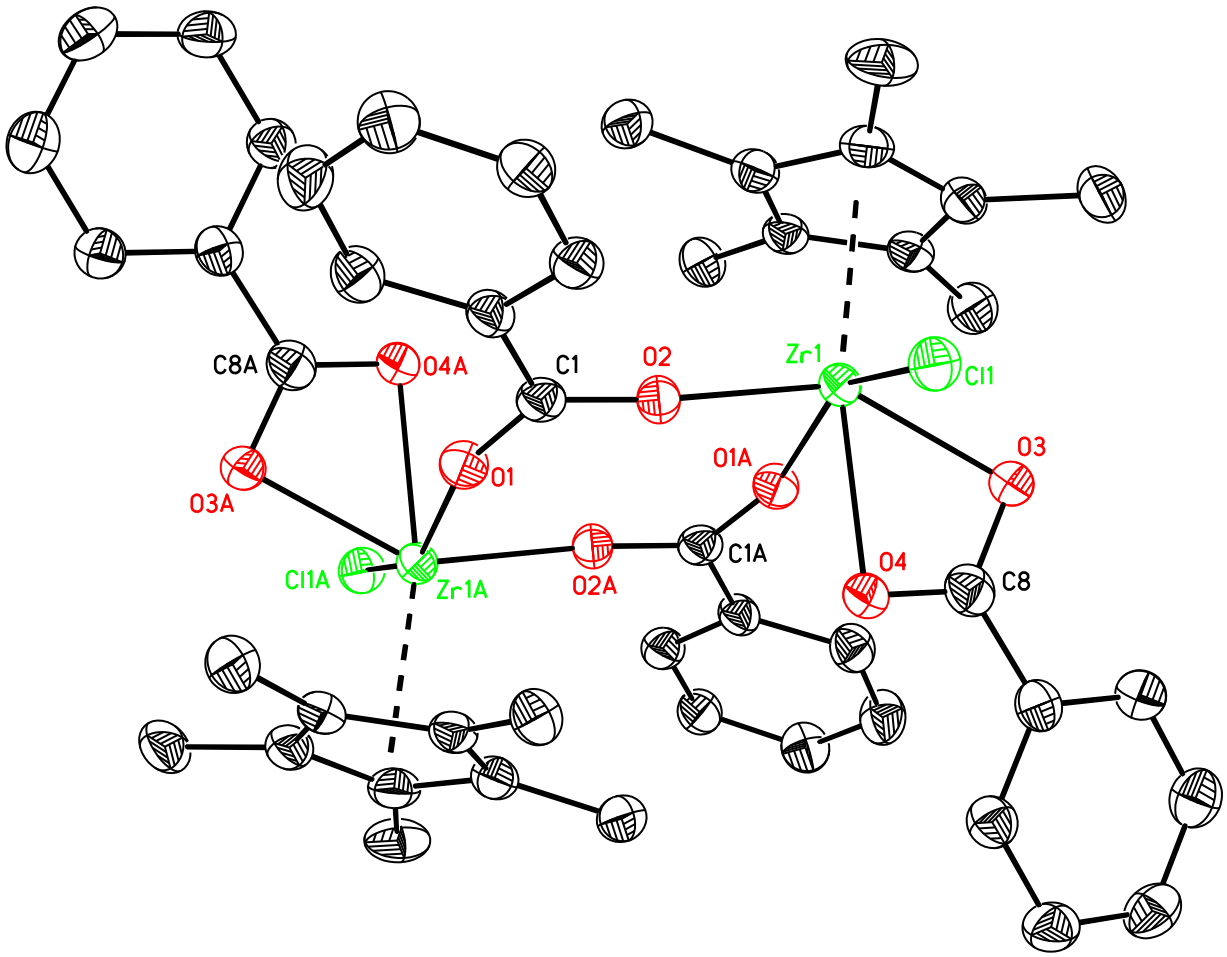


**Figure 2.** ORTEP drawing of **2** at 50% probability. H atoms are omitted for clarity.

The structure of compound **3•Et$_2$O** was refined to the triclinic space group of $\boldsymbol{P}_{-1}$. Similarly to **2**, two crystallographic independent Zr centers in **3** are coordinated by one Cp*, two O atoms from one chelating carboxylate group, and two O atoms from two bridging carboxylate moieties (Figure 3). The main difference in **3•Et$_2$O** when compared to species **2** is that the chlorides are replaced by bridging $\mu_2$-OH moieties, forming slightly distorted pentagonal bipyramids rather than octahedral species. As can be observed in the ORTEP structure, the chelated carboxylate groups face each other and can be considered "up", whereas the bridging carboxylate groups are considered as "down". One remarkable feature of **3** is the inclusion of one diethyl ether molecule

captured between the two carboxylate ligands pointing “up”, forming molecular tweezers. This ether molecule is stabilized mainly by a strong hydrogen bond between the $\mu_2$-OH and the O atom in ether, as shown in Figure 3. In order to better understand the nature of the interaction between **3** and $Et_2O$ in play in **3•Et$_2$O**, the crystallographic data were collected at various temperatures. All of the unit cell parameters have been shown to be sensitive to temperature, indicating its modest flexibility. While the three axes are directly proportional to temperature, the three angles, $\alpha$, $\beta$, and $\gamma$, are reversely proportional to temperature (see Table S1 for more details). The structure of **3** at 196K will be selected for the description of the bond lengths since its refinement is the most reliable.

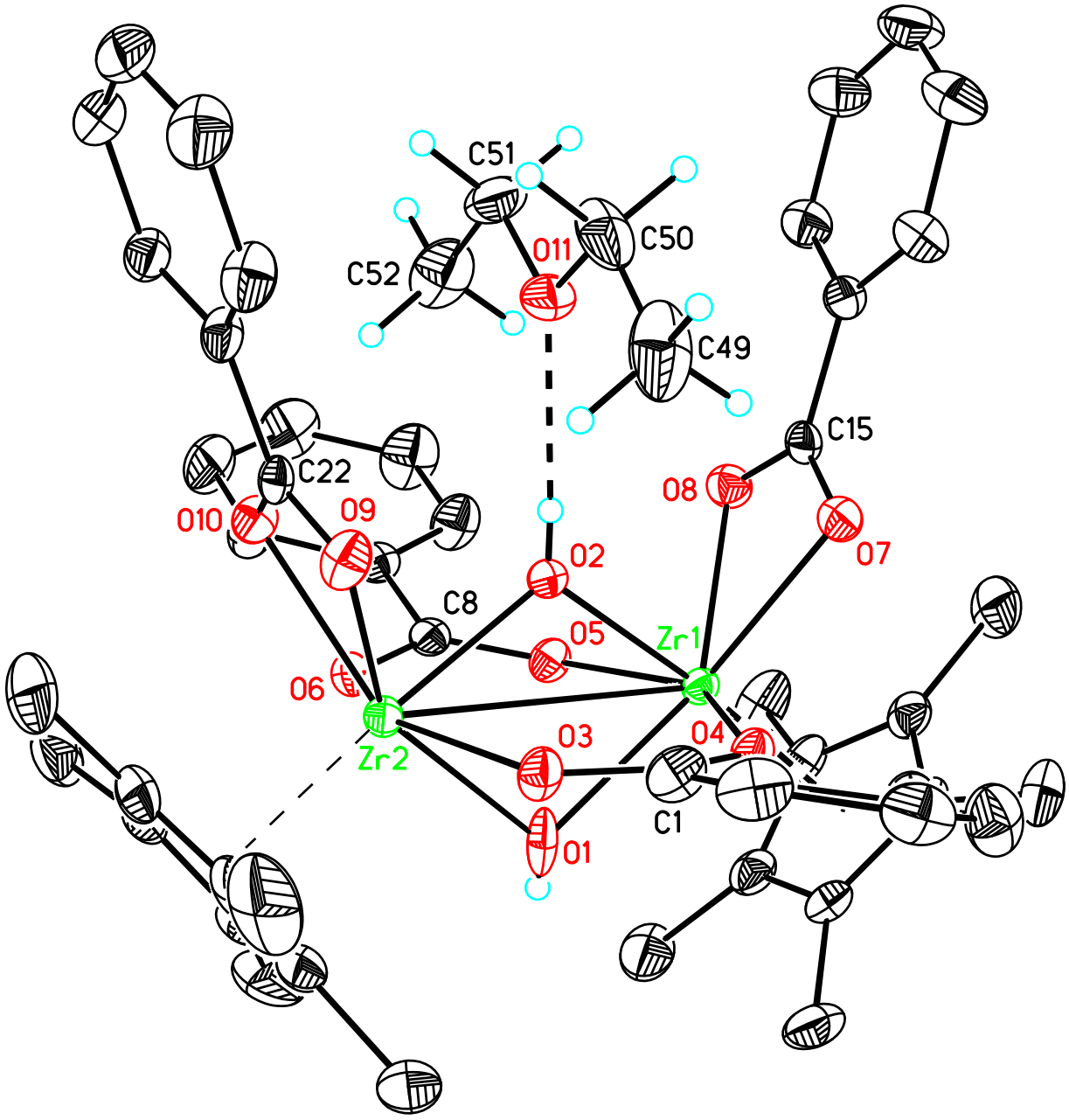


**Figure 3**. ORTEP drawing of **3.Et$_2$O** at 50% probability. H atoms on aromatic rings and Cp* are omitted for clarity.

In **3•Et$_2$O** the Zr-O bond lengths for the chelated carboxylates (Zr-O$_7$, Zr-O$_8$, Zr-O$_9$, Zr-O$_{10}$) range from 2.2763(16) to 2.3052(16) Å, which are comparable to those in **1** and **2**. Because of

the presence of two chelating $\mu_2$-OH fragments, the distance between $Zr_1$ and $Zr_2$ is much shorter than in **2**, at 3.4736(3) Å. The distances between the Zr atoms and the coordinated Cp* centres are of 2.2638(2) and 2.2601(2) Å, respectively. All the equatorial O atoms in the pentagonal bipyramids are pushed towards the vertex of $O_2$ (for example $O_2$-$Zr_1$-$O_4$ = 79.45(6), $O_2$-$Zr_1$-$O_5$ = 78.80(6), $O_2$-$Zr_1$-$O_1$ = 73.66(6), $O_2$-$Zr_1$-$O_8$ = 82.24(6), $O_2$-$Zr_1$-$O_7$ = 82.34(6)°). Interestingly, in the solid state structure, two molecules of **3** are arranged in a mouth-to-mouth fashion to form capsules with two ether molecules captured inside, as shown in Figure 4. The capsules are further linked to form chains along the 101 direction through weak π-π interactions between adjacent Cp* groups. The distance between two Cp* planes is 3.8695 Å.

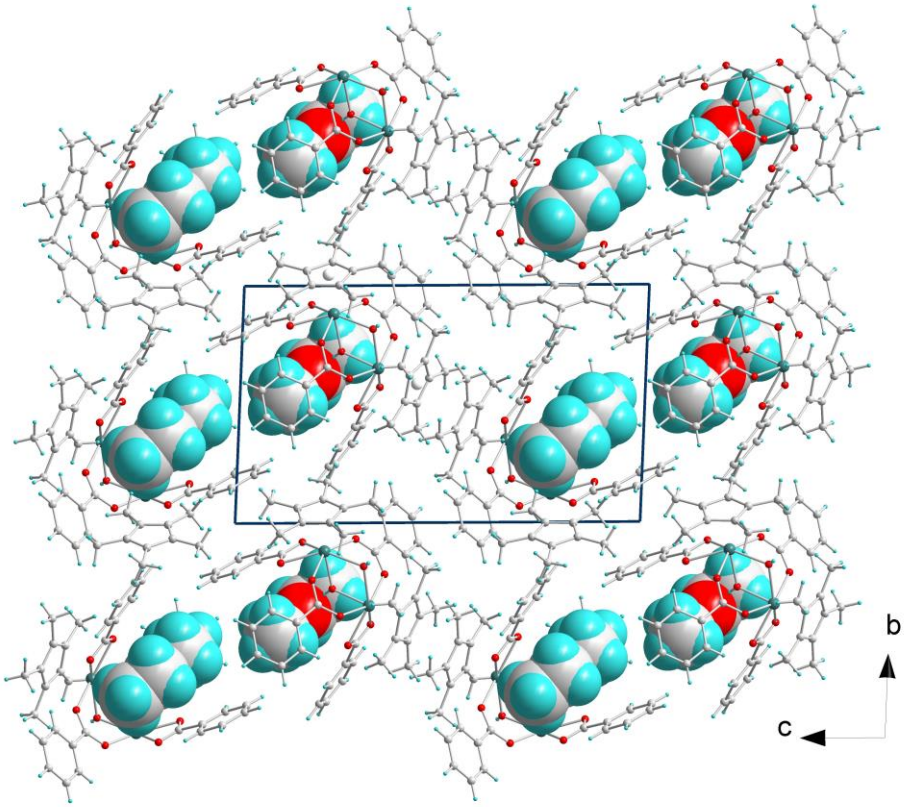


**Figure 4.** The packing pattern of **3** viewing along ***a*** axis. The guest molecules of diethyl ether are plotted in space filling mode.

At 200 K, the distance between $O_2$ and the $O_{11}$ atom of diethyl ether is only 2.763 Å with an interaction angle of 176.3 °, which would indicate a strong to moderate hydrogen bond.[18] As observed in Figure 5, the distance between the two oxygen atoms increases with temperature (2.742, 2.763, and 2.786 Å at 100, 196, and 296 K, respectively) therefore suggesting the weakening of the hydrogen bond with temperature. Although hydrogen bonding seems to be the primary interaction between **3** and $Et_2O$, other interactions seem to be present according to the crystallographic data. Indeed, the $C_{52}$-$O_{10}$, $C_{52}$-$O_8$, $C_{49}$-$O_9$, and $C_{49}$-$O_7$ distances (respectively of 3.552, 3.667, 3.502, and 3.673 Å) are short enough to consider possible interactions between the CH bonds of the methyl groups and the π system of the carboxylate moieties pointing "up". Such interactions would have for effect to decrease the coplanarity between the carboxylate moieties (O-C-O) and the phenyl ring in the phenylcarboxylate ligands, which is observed. Indeed, although the torsion between the aryl group and the OCO moiety is minimal (no twisting), there is folding present at the carboxylic carbon, as observed in Figure 6. The angles between the plane of the aryl group and the plane of the OCO moiety are respectively of 170.1 and 173.7° for the two chelating phenyl carboxylate groups pointing "up". This folding has also for effect to shorten the distances between the π rings and the C51 and C50 carbons, suggesting additional interactions. Once again, it is possible to observe that the interaction is stronger at lower temperature, as indicated by the aryl-aryl distance at the extremities of the chelating phenylcarboxylate ligands that is increasing with the temperature (8.300, 8.405, and 8.508 Å at 100, 196, and 296 K, respectively; Figure 5). It is good to note that this folding could be accounted by packing interactions and it is difficult to confirm if these secondary interactions are the cause of these structural changes.

Nevertheless, optimized structures of **3** with various solvents, including $Et_2O$ were obtained computationally by calculations based on the density of functional theory (DFT) using the ωB97XD functional.[19] Since these models are for the gas-phase, the crystal packing should not intervene in the structural parameters observed. As can be observed in Figure 7, significant structural changes are observed in the structure of the zirconium cluster between **3** and **3•Et₂O**. In the solvent-free structure, the central hydroxyl group is in a $sp^3$ environment, with the summation of the angles around the oxygen atom being of 336.6°, whereas the summation of the same angles in **3•Et₂O** is 357.5°. More importantly, there is significant folding between the Zr-OOC plane and the phenyl ring of the chelating phenylcarboxylate ("up") in the latter model, similarly to what was observed in the crystallographic structure. The average of the folding angles is 173.1° (170.1 and 173.7° in the structure) whereas the same angles have an average value of 178.1° in the solvent-free structure. The two bridging carboxylate moieties ("down") are more or less parallel to each other in the solvent-free molecule with an angle between the two phenyl rings being close to 180°; however, one of the phenylcarboxylate moiety is heavily distorted in the **3•Et₂O** model with a folding between the carboxylate plane and the phenyl ring of 126.6°, while the other has a respective angle of 167.4°. DFT supports that **3** is indeed greatly stabilized by interacting with $Et_2O$ since the $\Delta H°_{association}$ at the gas phase is -25.3 $kcal.mol^{-1}$ ($\Delta G°_{association}$ of -9.4 $kcal.mol^{-1}$). Interestingly, the association energies for **3** and THF and $Me_2O$ ($\Delta H°_{association}$ of -23.1 and -21.1 $kcal.mol^{-1}$, respectively) were found to be less important than with $Et_2O$, even if THF is known to be a better hydrogen bond acceptor, which suggest that the interactions between the CH bonds of the methyl groups and the π system of the carboxylate moieties pointing "up" are indeed playing a significant role on the stability of the adduct, as proposed above. $SMe_2$ does not seem to interact with the cavity, which can be expected since

sulfur does not form hydrogen bonds as strongly as oxygen. More details are given in the Supporting Information.

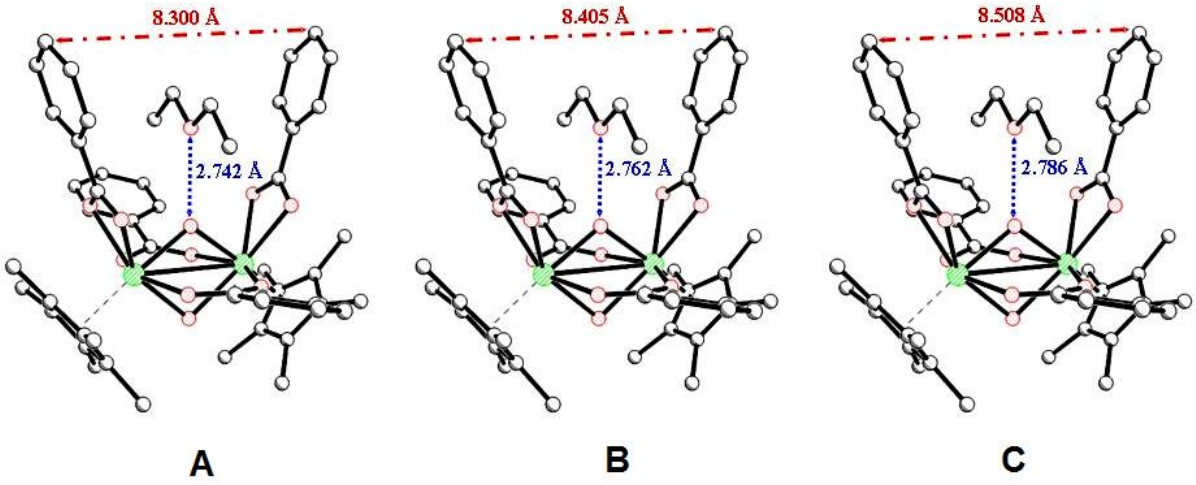


**Figure 5.** Important structural data for the structure of **3.Et$_2$O** at A) 100K, B) 196K, and C) 296 K.

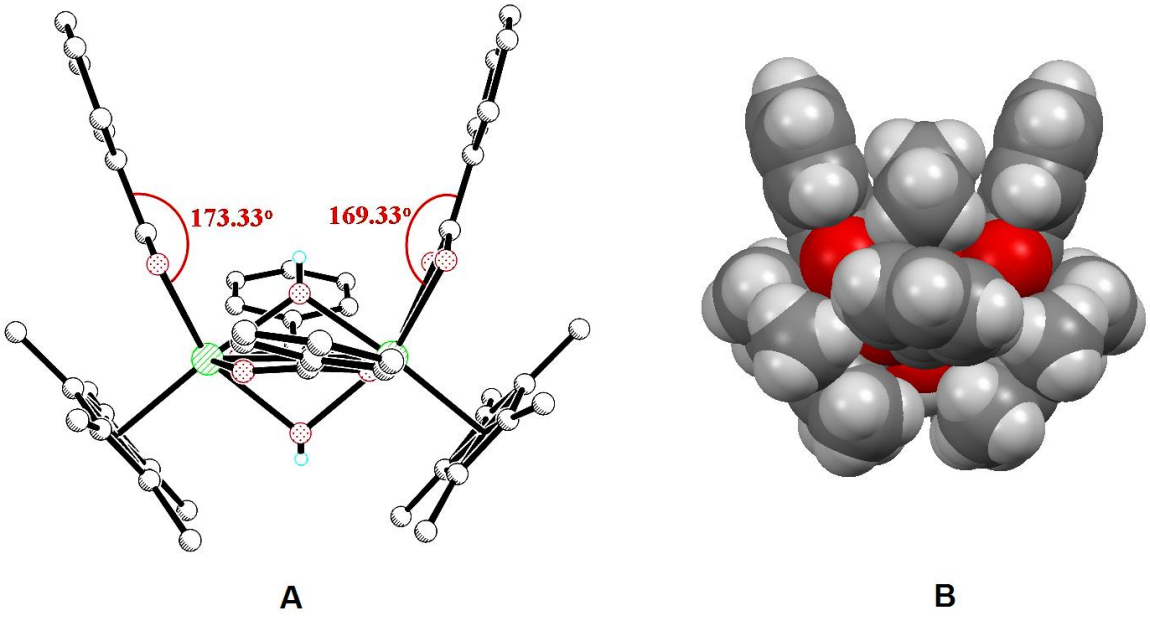

**Figure 6**. A) Representation of the folding observed in the phenylcarboxylate ligands and B) space filling representation of species **3.Et$_2$O**.

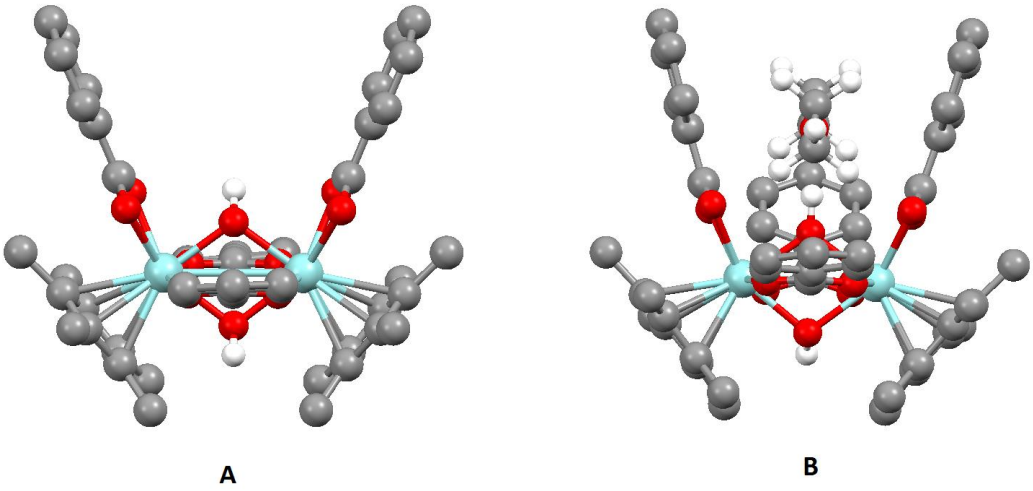


**Figure 7**. Computationally optimized gas-phase models for A) **3** and B) **3.Et$_2$O**. These results were obtained using the ωB97XD functional and the 6-31G**[20] basis set for C, H and O atoms and the SDD basis set for Zr.[21]

In order to see the effect of the water stoichiometry on the products formed, the same reaction was carried out, this time using two equivalents of water rather than only one (Scheme 4). In this situation, few crystals of the tetrametallic product [[Cp*ZrCl$_2$](μ-Cl)(μ-OH)(μ-O$_2$CC$_6$H$_5$)[Cp*Zr]]$_2$(μ-O$_2$CC$_6$H$_5$)$_2$ (**4**) were observed, enough for a crystallographic study but not for a full characterization, along with a significant amount of amorphous material. Due to the low crystallinity, the hydrogen atoms on the $\mu_2$-OH could not be located from the differential Fourier map. It crystalized in the central symmetric space group of P2$_1$/c, with a very long ***b*** axis of 38.8446(5) Å. There are two independent molecules present in the unit cell, with one of the two molecules being located on an inversion centre, which makes half of that molecule symmetric to the other half. As shown in the ORTEP representation in Figure 8 for one of the

two independent molecules, the polymetallic species consists of one $Cp^*ZrCl_2$ fragment bridging another Cp*Zr moiety by one chloride, one hydroxide, and one carboxylate group. Two of these bimetallic moieties are bridged together by two carboxylate groups; in one of these two independent molecules only one half of the molecule moiety is included in the asymmetric unit cell, the other half being generated by the inversion centre. All of the zirconium centres are in a pseudo-octahedral environment with the substituents being pushed away from the bulkiest group, the Cp*. One benzene ring is captured in the structure.

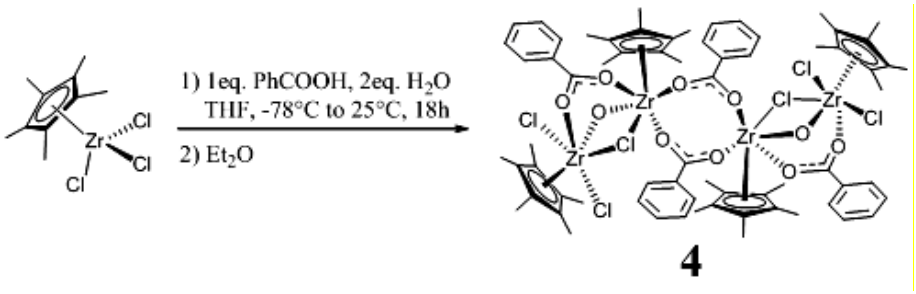


**Scheme 4:** Synthesis of complex $[[Cp^*ZrCl_2](\mu\text{-}Cl)(\mu\text{-}OH)(\mu\text{-}O_2CC_6H_5)[Cp^*Zr]]_2(\mu\text{-}O_2CC_6H_5)_2$ (**4**)

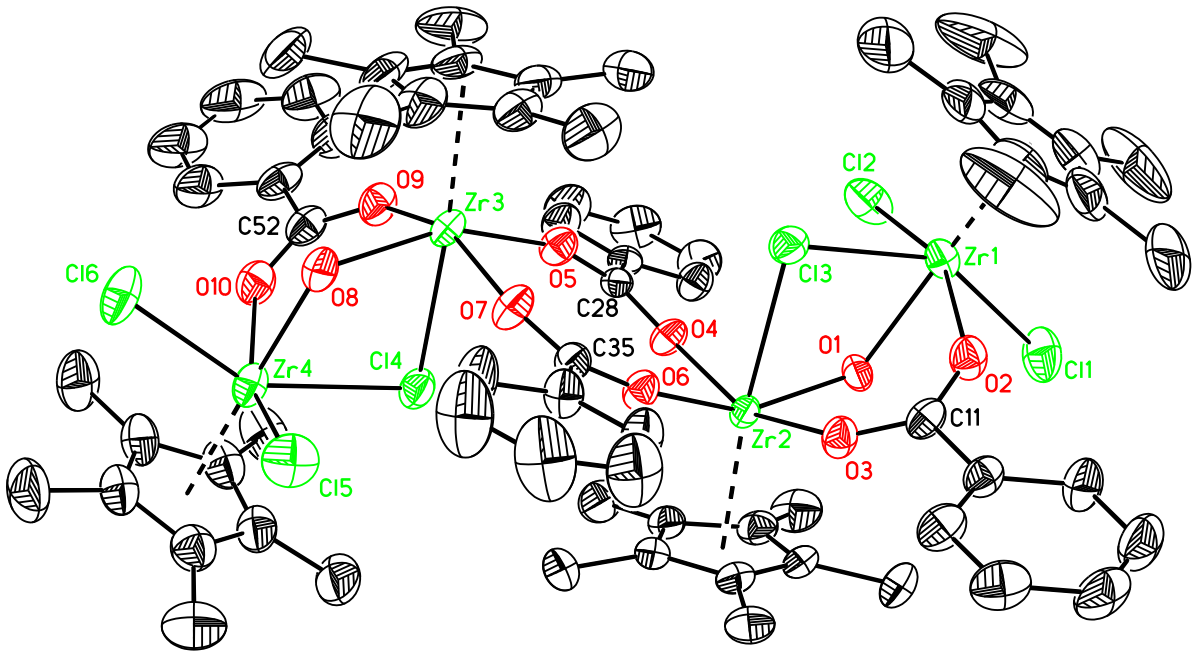

**Figure 8.** ORTEP drawing of **4** at 50% probability. One of the two independent molecules is shown. H atoms were are omitted for clarity.

The distances between the centres of the Cp* planes and the Zr atoms range from 2.2250(5) to 2.2543(4) Å, which are longer than that in **2**, but are comparable to those in **1**. The terminal Zr-Cl bond lengths range from 2.4498(20) to 2.4892(20) Å. Due to the existence of $\mu_2$-OH, the short Zr-Zr distances range from 3.7665(7) ($Zr_1$-$Zr_2$) to 3.7880(6) ($Zr_5$-$Zr_6$) Å, which are longer than that observed in **3** (3.4736(3) Å). However, the long Zr-Zr distances ($Zr_2$-$Zr_3$ = 5.2172(7), $Zr_5$-$Zr_{5'}$ = 5.2212(6) Å) are comparable to that observed in **2** (5.2146(13) Å). The 3D network is illustrated in Figure S17.

All our attempts to generate a metallocavitand reminiscent to the one observed using the CpZr(IV) moiety failed using phenylcarboxylic acid. However, it is known that simple modifications in the nature of the ligands can affect the structure of the complexes obtained. Using more acidic 4-bromophenylcarboxylic acid in similar conditions rather than phenylcarboxylic acid, it was possible to observe the formation of ionic species $[(Cp^*Zr)_3(\kappa_2\text{-}O',O''C(C_6H_4Br)_3(\mu_3\text{-}O)(\mu_2\text{-}Cl)_2(\mu_2\text{-}O\mathit{H})]^+$ $[Cp^*ZrCl_4]^-$ (**[5]**$^+$[**Cp*ZrCl$_4$**]$^-$) which is isostructural to the coveted metallocavitands. According to the charge balance, there should be the presence of one hydroxide in the trimetallic cluster; however, it was not possible to locate the position of the hydrogen atom, making difficult an unambiguous assignment of the hydroxide group (Figure 9). Close contact between the cation **5** and the $Cp^*ZrCl_4^-$ anion is mainly occurring through electrostatic interactions between the bromine in *para* position of the aryl groups and the anion, as represented in Figure S21. The ion pairs are linked into layers in the *a*-*c* plane, with the layers

packed together along the *b* axis via π-π interactions between the Cp* planes from adjacent **5** units (Figures S19-S20).

The coordination environment around the metal center in the $[Cp^*ZrCl_4]^-$ anion is square pyramidal, with the metal center being 0.8289 Å from the plane composed by the four chloride ligands. The Cp*-Zr distance is relatively short, at 2.1914(10) Å and the Zr-Cl distances range from 2.453(3) to 2.486(3) Å. However, the main species of interest, the cationic **5** consists in a trimetallic cluster where the three Cp*Zr moieties are linked together by one $\mu_3$-O atom, one $\mu_2$-OH group, two $\mu_2$-Cl atoms, and three carboxylate groups to form a cluster like in $[(CpZr)_3(\mu\text{-}\kappa_2,O',O''CR)_3(\mu_3\text{-}O)(\mu_2\text{-}OH)_3]Cl$. Due to the special geometry of this cluster, the three carboxylate groups form the edge of a bowl, with the metallic cluster forming the bottom.

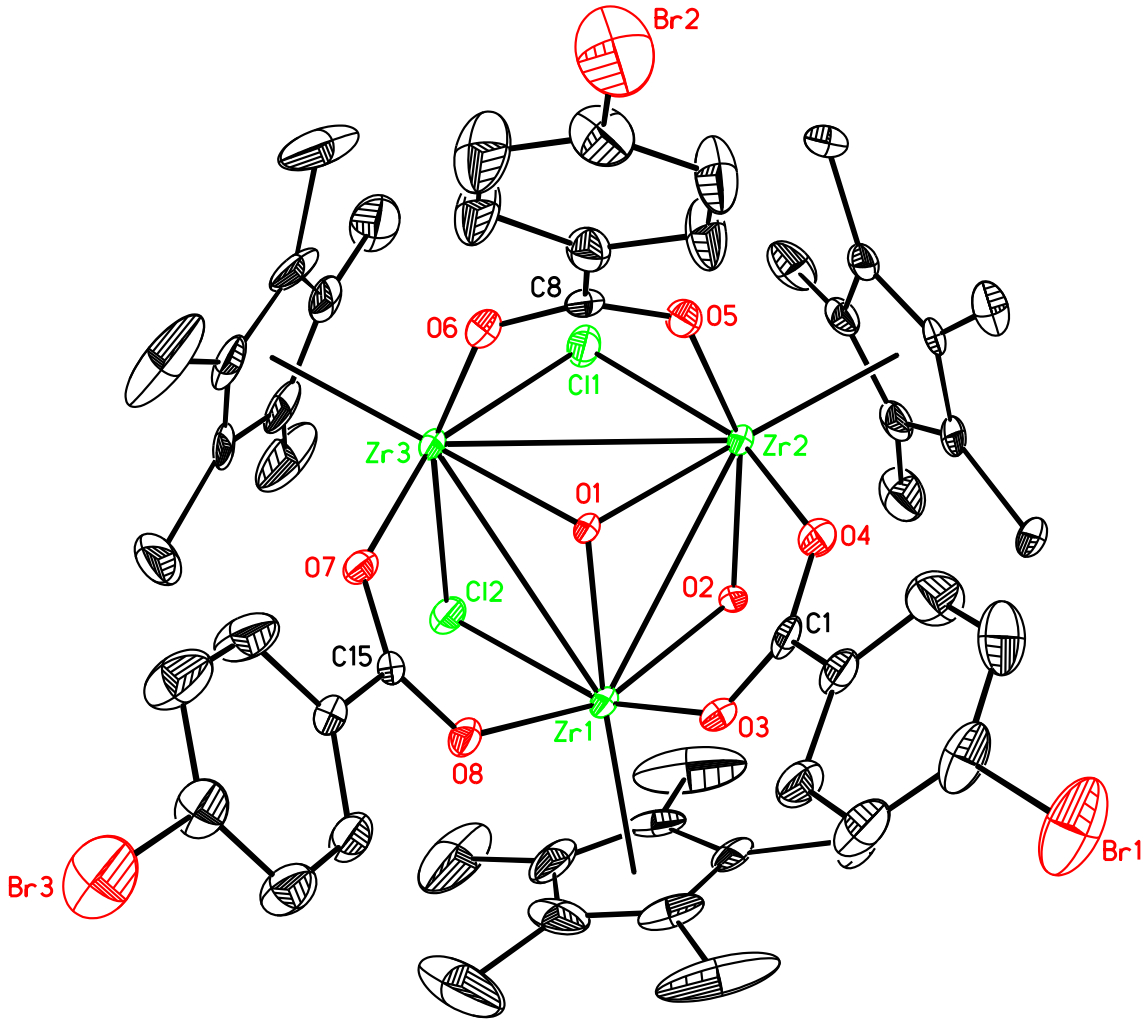


**Figure 9.** ORTEP drawing of **[5]**$^{+}$ at 50% probability. H atoms are omitted for clarity.

The Zr-($\mu_2$-OH) distances are of 2.180(7) and 2.190(6) Å, respectively, which are as expected for a bridging hydroxide group. Indeed, Roesky and co-workers reported that average Zr-O bond lengths for bridging Zr-OH-Zr moieties are around 2.16 Å whereas the analogous bond lengths for bridging oxide Zr-O-Zr are shorter, varying between 1.945 and 2.106 Å.[22] Following the same report, a $\mu_3$-O can be proposed since the Zr-($\mu_3$-O) average bond length in **5** (2.102 Å) is close the expected trend (2.060 and 2.095 Å) for such bridging oxide, whereas bridging hydroxides will have bond lengths between 2.170 and 2.410 Å. As expected by the presence of

the two bridging chlorides, **5** does not show a $C_3$ symmetry but rather possesses a single pseudo-plane of symmetry. That can be observed by the presence of two long Zr-Zr distances (3.5557(11) and 3.5806(11) Å) and of one shorter (3.4164(12) Å). The lower symmetry can also be observed in solution where several sets of resonances for the 4-bromobenzoate are observed. The possibility of further fluxional process in solution is not overlooked since two sharp Cp* are observed at 2.09 and 2.17 ppm, along with one broader resonance at 2.26 ppm when crystals of **5** are put in solution. The Cp*-$Zr_3$-($\mu_3$-O) angle for the metal binding two chlorides is of 177.3° whereas the respective Cp*-Zr-($\mu_3$-O) angles for the species binding one chloride are of 174.8° in average. Accordingly, the Zr-Cl-Zr angles are of 87.5° whereas the Zr-OH-Zr angle is of 102.8°. These results suggest that the more important volume of the chloride anion has for effect to push it away from the metallic core, thereby reducing the Zr-Cl-Zr angles. That steric bulk caused by the chloride has also for effect to give one narrow Zr-($\mu_3$-O)-Zr angle of 108.0°, for the metallic centres bridging the hydroxide, and two wider Zr-($\mu_3$-O)-Zr angles of 116.1 and 116.9° for the metallic centre bridging the chlorides.

The presence of π-π interactions is significant in the crystal lattice. Indeed, it can be observed that two molecules of **5** will interact with each other by interactions through Cp* moieties, as demonstrated by such a distance of 3.72 Å. No inclusion species were observed in the crystal structure of **5**, but the void of the cavity was shown to be filled by stacking of the metallocavitands into each other, as shown in Figure 10. This stacking was notably observed in tantalum metallocavitands previously reported by our research group.[10a]

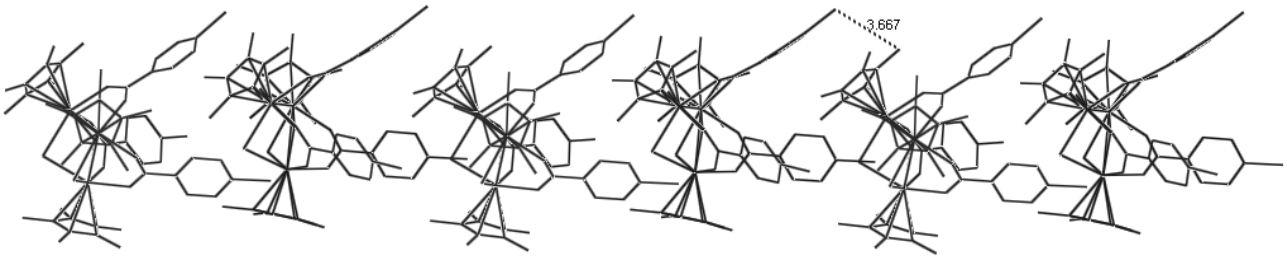


**Figure 10.** Stacking of species **5**.

## Conclusion

Although the synthesis of Cp*Zr carboxylate species has been reported previously, the direct synthesis of the zirconium compounds from carboxylic acids and the $Cp^*ZrCl_3$ precursor was never reported, to the best of our knowledge. As expected, the chemistry observed with the more bulky and electron-rich pentamethylcyclopentadienyl ligand is quite different from the one observed with the Cp-derivatives. The coordination modes of the novel species structurally characterized are very dependent on the reaction conditions, the nature of the solvent, the modification of the phenylcarboxylic acid, and in the number of equivalents of water added during the synthesis. Out of the five crystallographic structures that were obtained, two are of notable interest. Species **3** exhibits host-guest characteristics with diethyl ether, which greatly modify the structural parameters of this cluster. The hydrogen bonding and the CH-π contacts were not only observed at the solid-state, but also in the gas-phase models using DFT methods. It was also possible to isolate one of the desired metallocavitand using the 4-Br-phenylcarboxylate ligand but we have not been successful yet in replacing the bridging chlorides with bridging oxo/hydroxide ligands as it was observed for the CpZr(IV) and Cp*Ta(V) clusters previously reported by our research group.[10,11] We are currently looking at extending this chemistry and at discovering interesting properties for these metallocavitands notably for host-guest interactions.

## Experimental section

### General Procedure

Syntheses and subsequent work-up of the zirconium clusters were conducted under an atmosphere of nitrogen using standard glovebox techniques. Toluene, DME, THF, ethyl ether were purified over Na/benzophenone. Benzene-$d_6$ and $CHCl_3$ were purified by vacuum distillation from Na/K alloy and vacuum transfer technique respectively. $Cp^*ZrCl_3$[16] and $Cp^*_2ZrCl_2$[23] were prepared according to literature procedures. Carboxylic acids were purchased from Aldrich and used as received. NMR spectra were recorded on an Agilent Technologies NMR spectrometer at 500 MHz ($^1H$), 125.758 MHz ($^{13}C$) or a Varian Inova NMR AS400 spectrometer, at 400.0 MHz ($^1H$), 100.580 MHz ($^{13}C$). $^1H$ NMR and $^{13}C$ NMR chemical shifts are referenced to residual protons or carbons in deuterated solvent. HRMS data were collected by the Mass Spectrometry Facilities at Laval University with an Agilent 6210 Time-of-Flight (TOF) LC-MS apparatus equipped with a ESI or APPI ion source (Agilent Technologies, Toronto, Canada).

### Synthesis of $Cp^*_2ZrCl(\kappa^2\text{-}OOCPh)$ (1)

A solution of benzoic acid (0.112 g, 1.0 mmol) in water (5mL, pH = 7-8) was added to a solution of $Cp^*_2ZrCl_2$ (0.432 g, 1.0 mmol) and stirred at room temperature for 18h. The organic layer was extracted 3 times (10mL) with $CH_2Cl_2$. The organic phases were combined, washed with brine and dried over $MgSO_4$. Once filtered, the organic phase was evaporated under vacuum which yield to a white powder (0.200 mg, 39%). $^1H$ NMR (400 MHz, $CDCl_3$) $\delta$ 8.11 (d, $^3J_{H\text{-}H}$ = 7.2 Hz, 2H), 7.55 (t, $^3J_{H\text{-}H}$ = 7.3 Hz, 1H), 7.44 (t, $^3J_{H\text{-}H}$ = 7.5 Hz, 2H), 1.88 (s, 30H). $^{13}C$ NMR (101 MHz, cdcl$_3$) δ 177.6, 133.0, 132.1, 129.4, 128.4, 121.8, 11.7. Exact mass calculated: $C_{27}H_{35}ClO_2Zr$ $[M\text{-}H_3O^+]^+$ 535.1557. Found : m/z $[M\text{-}H_3O^+]^+$ : 535.5170.

**Synthesis of $Cp^*ZrCl(\kappa^2\text{-}OOCPh))_2(\mu\text{-}\kappa^2\text{-}OOCPh)_2$ (2) and $[(Cp^*Zr(\kappa^2\text{-}OOCPh))_2(\mu\text{-}\kappa^2\text{-}OOCPh)_2(\mu^2\text{-}OH)_2]\bullet Et_2O$ (3•$Et_2O$) (3)**

A solution of benzoic acid (22 mg, 0.18 mmol) and deionized water (1.6 μL, 0.09 mmol) in THF (3 mL) was added at -78 °C to a solution of $Cp^*ZrCl_3$ (30 mg, 0.09 mmol) in THF (3 mL). The resulting yellow solution was stirred at 70°C for 18h. The solvent was then removed under reduced pressure to obtain a blue solid. 5 mL of diethyl ether were added and a colorless solution was obtained and stirred for 3 hour at room temperature until a white precipitate crash out from the solution. The white precipitate was filtered and washed 3 times with cold diethyl ether and dried under vacuum to yield (37 mg, 71% m/m). Crystals of $Cp^*ZrCl(\kappa^2\text{-}OOCPh))_2(\mu\text{-}\kappa^2\text{-}OOCPh)_2$ and $[(Cp^*Zr(\kappa^2\text{-}OOCPh))_2(\mu\text{-}\kappa^2\text{-}OOCPh)_2(\mu^2\text{-}OH)_2]\bullet Et_2O$ were obtained from slow evaporation of a solution in diethyl ether and were handpicked for crystallographic analysis. The solution characterization of **2** was not possible because of the lack of material. $^1$H RMN $[(Cp^*Zr(\kappa^2\text{-}OOCPh))_2(\mu\text{-}\kappa^2\text{-}OOCPh)_2(\mu^2\text{-}OH)_2]\bullet Et_2O$ (benzene-$d_6$): $\delta$ 8.17 (br d, $^3J_{H\text{-}H}$ = 7.4 Hz, 3H), 8.09 (br d, $^3J_{H\text{-}H}$ = 7.8 Hz, 1H), 8.04 (br d, $^3J_{H\text{-}H}$ = 7.5 Hz, 2H), 7.97 (br d, $^3J_{H\text{-}H}$ = 8.1 Hz, 1H), 7.18 (br s, 1H), 7.16 (br s, 1H), 7.12-7.06 (br m, 6H), 6.99-6.95 (br m, 1H), 2.06 (s, 15H), 2.03 (s, 15H), 1.90 (s, 1H). $^{13}$C NMR (101 MHz, $C_6D_6$) δ 181.5, 133.9, 133.4, 132.5, 129.7, 129.4, 128.9, 128.7, 128.1, 126.3, 123.7, 123.5, 121.7, 65.9 ($Et_2O$), 15.6 ($Et_2O$), 12.3, 11.7, 10.7. Exact mass calculated $C_{52}H_{62}O_{11}Zr_2$ [M-$Et_2$O-O+] : 952.1705. Found: m/z [M-$Et_2$O-O+]+ : 952.1633.

**Synthesis of $[[Cp^*ZrCl_2](\mu\text{-}Cl)(\mu\text{-}OH)(\mu\text{-}O_2CC_6H_5)[Cp^*Zr]]_2(\mu\text{-}O_2CC_6H_5)_2$ (4)**

A solution of benzoic acid (23 mg, 0.18 mmol) and deionized water (6.9 μL, 0.384 mmol) in THF (5 mL) was added at -78 °C to a solution of $Cp^*ZrCl_3$ (64 mg, 0.19 mmol) in THF (5 mL). The resulting solution was stirred at room temperature for 18h. The solvent was then removed under reduced pressure to obtain a blue solid. 10 mL of diethyl ether were added and no precipitate was observed after stirring 48h at room temperature. Ethyl ether was evaporated and 5mL of hexane were added. A white precipitate was observed then filtered. Few crystals were collected from the evaporation of a benzene solution along with degradation material. These crystals were subjected to X-ray analysis.

**$[Cp^*ZrCl_4][(Cp^*Zr)_3(\kappa_2\text{-}O',O''C(C_6H_4Br)_3(\mu_3\text{-}O)(\mu_2\text{-}Cl)_2(\mu_2\text{-}O\mathit{H})]$ $Cp^*ZrCl_4$ (5)**

A solution of 4-bromobenzoic acid (248 mg, 1.23 mmol) and deionized water (11.1 μL, 0.616 mmol) in THF (10 mL) was added at -78 °C to a solution of $Cp^*ZrCl_3$ (205 mg, 0.616 mmol) in THF (10 mL). The resulting yellow solution was stirred at 80 °C for 24h. The solvent was then removed under reduced pressure to obtain a reddish solid. 5 mL of acetonitrile was added from which a white solid precipitated. The solution was filtered and the filtrate was allowed to crystallize for 1 month. The dried residue was dissolved in benzene from which a yellow precipitate was filtered out. Yellow crystals were obtained from slow evaporation in chloroform and THF (50:50) (79 mg, 21%), $^1$H NMR (400 MHz, $CDCl_3$) δ 7.72(d, $^3J_{H\text{-}H}$ = 8.1 Hz, 3H), 7.62(d, $^3J_{H\text{-}H}$ = 8.5 Hz, 1H), 7.54 (d, $^3J_{H\text{-}H}$ = 8.1 Hz, 3H), 7.42 (d, $^3J_{H\text{-}H}$ = 8.3 Hz, 2H), 7.27 (d, $^3J_{H\text{-}H}$ = 8.3 Hz, 2H), 6.37 (s, 1H), 2.26-2.09 (m, 60H). $^{13}$C NMR (101 MHz, $CDCl_3$) δ 138.0, 132.3, 131.3, 130.2, 128.1, 127.8, 127.6, 126.6, 110.0, 12.4, 12.1. Exact mass calculated: $C_{51}H_{58}Br_3Cl_2O_8Zr_3^+$: 1382.822. Found: m/z [M]+ :1382.6637.

**Crystallographic data**

Single crystals with suitable size of all compounds were mounted on CryoLoops with Paratone-N and optically aligned on a Bruker SMART APEX-II X-ray diffractometer with 1K CCD detector using a digital camera. Initial intensity measurements were performed using a fine-focused sealed tube, graphite-monochromated, X-ray source (Mo $K\alpha$, $\lambda$ = 0.71073 Å) at 50 kV and 30 mA. Standard APEX-II[24] software package was used for determining the unit cells, generating the data collection strategy, and controlling data collection. SAINT[25] was used for data integration including Lorentz and polarization corrections. Semi-empirical absorption corrections were applied using SCALE (SADABS).[26] The structures of all compounds were solved by direct methods and refined by full-matrix least-squares methods with SHELX-97[27] in the SHELXTL6.14 package. As the solvent molecules in some compounds are highly disordered, the SQUEEZE subroutine of the PLATON[28] software suit was used to remove the scattering contributions from the highly disordered guest molecules. The resulting new HKL files were used to further refine the structures. All of the H atoms (on C atoms) were generated geometrically and refined in riding mode. Crystallographic information for all obtained phases is summarized in Table S1. Atomic coordinates and additional structural information are provided in the cif files of the Supporting Information.

**Computational details**

Calculations were performed with the GAUSSIAN 09 suite of programs.[29] The ωb97xd[19] functional was used in combination with the 6-31G* basis set for C, H, O and S atoms[20] and the SDD basis set for the Zr atom.[21] The stationary points were characterized as minima by full vibration frequencies calculations (no imaginary frequency). All geometry optimizations were

carried out without any symmetry constraints. All structures with their associated free enthalpy and Gibbs free energies as well as their cartesian coordinates are fully detailed in the Supplementary Information Section.

**Supporting Information Available:** NMR spectra of species **1**-**5,** additional crystallographic figures and DFT details are available. This material is available free of charge via the Internet at http://pubs.acs.org. Crystallographic data have been deposited with CCDC (CCDC No. 1054618 for **1**, CCDC No. 1054619 for **2**, CCDC No. 1054620 for **3** (100 K), CCDC No. 1054621 for **3** (196 K), CCDC No. 1054626 for **3** (296 K), CCDC No. 1054732 for **4**, and CCDC No. 1054625 for **5**). These data can be obtained upon request from the Cambridge Crystallographic Data Centre, 12 Union Road, Cambridge CB2 1EZ, UK, e-mail: deposit@ccdc.cam.ac.uk, or via the internet at www.ccdc.cam.ac.uk.

**Acknowledgment.** We are grateful to FQRNT (Projet de recherche en équipe - Québec) and CFI (Canada), CCVC (Québec), and CQMF (Québec) for financial support. M.-A.L is grateful to the NSERC for a scholarship. We acknowledge the help of Pierre Audet with the HR-MS experiments.

**Table of Contents Graphic**

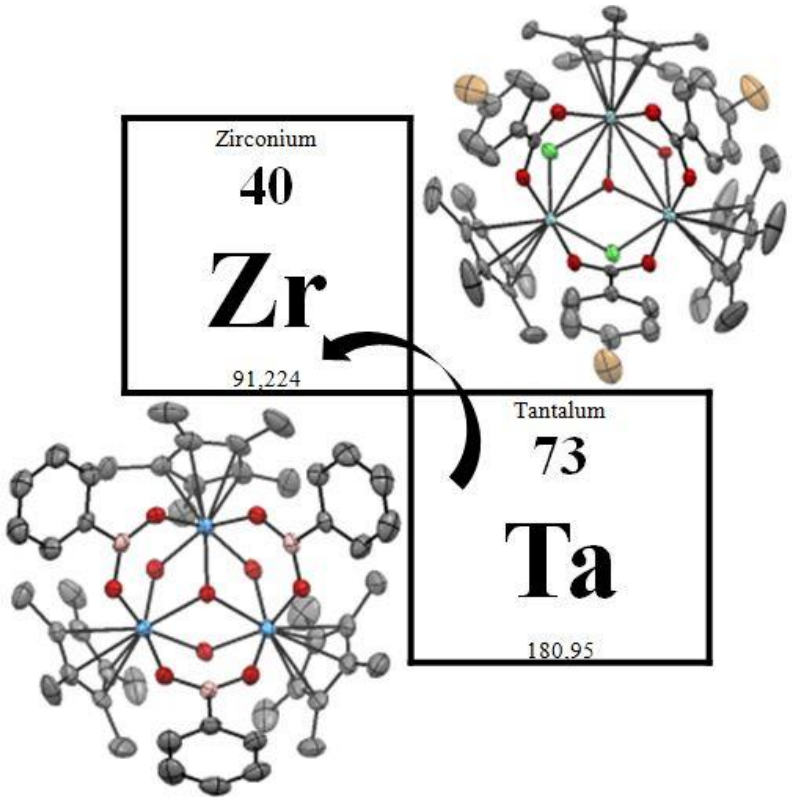


**Table of Contents Synopsis**

The reaction of $Cp^*_2ZrCl_2$ and $Cp^*ZrCl_3$ with phenylcarboxylic acids was carried out. Depending on the reaction conditions, five new complexes were obtained, which consisted of $Cp^*_2ZrCl(\kappa^2\text{-}OOCPh)$ (**1**), $(Cp^*ZrCl(\kappa^2\text{-}OOCPh))_2(\mu\text{-}\kappa^2\text{-}OOCPh)_2$ (**2**), $[(Cp^*Zr(\kappa^2\text{-}OOCPh))_2(\mu\text{-}\kappa^2\text{-}OOCPh)_2(\mu^2\text{-}OH)_2]\bullet Et_2O$ (**3•Et₂O**), $[[Cp^*ZrCl_2](\mu\text{-}Cl)(\mu\text{-}OH)(\mu\text{-}O_2CC_6H_5)[Cp^*Zr]]_2(\mu\text{-}O_2CC_6H_5)_2$ (**4**) and $[Cp^*ZrCl_4][(Cp^*Zr)_3(\kappa_2\text{-}O',O''C(C_6H_4Br)_3(\mu_3\text{-}O)(\mu_2\text{-}Cl)_2(\mu_2\text{-}O\mathit{H})]$ [**Cp*ZrCl₄**][**5**]. Species **3•Et₂O** exhibits host-guest properties where the diethyl ether molecule is included in a cavity formed by two carboxylate moieties. Species **5** was shown to be isostructural to the $[(CpZr)_3(\mu^3\text{-}O)(\mu^2\text{-}OH)_3(\kappa_{O,O},\mu^2\text{-}O_2C(R))_3]^+$ metallocavitands.

**References**


[1] a) Mahon, C. S.; Fulton, D. A. *Nature Chem.* **2014**, *6*, 665-672. b) Pinalli, R.; Dalcanale, E. *Acc. Chem. Res.* **2013**, *46*, 399-411. c) Uhlenheuer, D. A.; Petkau, K.; Brunsveld, L. *Chem. Soc. Rev.* **2010**, *39*, 2817-2826. d) Huerta, E.; Metselaar, G. A.; Fragoso, A.; Santos, E.; Bo, C.; de Mendoza, J. *Angew. Chem. Int. Ed.* **2007**, *46*, 202-205. e) Eckert, J.-F.; Byrne, D.; Nicoud, J.-F.; Oswald, L.; Nierengarten, J.-F.; Numata, M.; Ikeda, A.; Shinkai, S.; Armaroli, N. *New J. Chem.* **2000**, *24*, 749-758. f) Lehn, J.-M. *Angew. Chem. Int. Ed. Engl.* **1990**, *29*, 1304-1319.

[2] a) Leenders, S. H. A. M.; Gramage-Doria, R.; de Bruin, B.; Reek, J. N. H. *Chem. Soc. Rev.* **2015**, *44*, 433-448. b) Leigh, D. A.; Marcos, V.; Wilson, M. R. *ACS Cat.* **2014**, *4*, 4490-4497. c) Ballester, P.; Vidal-Ferran, A.; van Leeuwen, P. W. N. M. *Adv. Catal.* **2011**, *54*, 63-126. d) Hooley, R. J.; Rebek Jr., J. *Chem. Biol.* **2009**, *16*, 255-264. e) Pinacho Crisóstomo, F. R.; Lledó, A.; Shenoy, S. R.; Iwasawa, T.; Rebek, Jr. J. *J. Am. Chem. Soc.* **2009**, *131*, 7402-7410.

[3] a) Higler, I.; Timmerman, P.; Verboom, W.; Reinhoudt, D. N. *Eur. J. Org. Chem.* **1998**, 2689-2702. b) Cram, D. J. *Science* **1983**, *219*, 1177-1783.

[4] a) Redshaw, C. *Coord. Chem. Rev.* **2003**, *244*, 45-70. b) Matthews, S. E.; Beer, P. D. *Supramol. Chem.* **2005**, *17*, 411-435.

[5] a) Pemberton, B. C.; Raghunathan, R.; Volla, S.; Sivaguru, J. *Chem. Eur. J.* **2012**, *18*, 12178-12190. b) Lee, J. W.; Samal, S.; Selvapalam, N.; Kim, H.-J.; Kim, K. *Acc. Chem. Res.* **2003**, *36*, 621-630. c) Yi, J.-M.; Zhang, Y.-Q.; Cong, H.; Xue, S.-F.; Tao, Z. *J. Mol. Struct.* **2009**, *933*, 112-117.

[6] a) Hardie, M. J. *Chem. Soc. Rev.* **2010**, *39*, 516-527. b) Matsubara, H.; Oguri, S.-y.; Asano, K.; Yamamoto, K. *Chem. Lett.* **1999**, *28*, 431-432.

[7] a) Liu, Y.; Chen, Y. *Acc. Chem. Res.* **2006**, *39*, 681-691. b) Hapiot, F.; Tilloy, S.; Monflier, E. *Chem. Rev.* **2006**, *106*, 767-781. c) Jeon, W. S.; Moon, K.; Park, S. H.; Chun, H.; Ko, Y. H.; Lee, J. Y.; Lee, E. S.; Samal, S.; Selvapalam, N.; Rekharsky, M. V.; Sindelar, V.; Sobransingh, D.; Inoue, Y.; Kaifer, A. E.; Kim, K. *J. Am. Chem. Soc.* **2005**, *127*, 12984-12989.

[8] Azov, V. A.; Beeby, A.; Cacciarini, M.; Cheetham, A. G.; Diederich, F.; Frei, M.; Gimzewski, J. K.; Gramlich, V.; Hecht, B.; Jaun, B.; Latychevskaia, T.; Lieb, A.; Lill, Y.; Marotti, F.; Schlegel, A.; Schlittler, R. R.; Skinner, P. J.; Seiler, P.; Yamakoshi, Y. *Adv. Funct. Mater.* **2006**, *16*, 147-156.

[9] a) Lenthall, J. T.; Steed, J. W. *Coord. Chem. Rev.* **2007**, *251*, 1747-1760. b) Frischmann, P. D.; MacLachlan, M. J. *Comments Inorg. Chem.* **2008**, *29*, 26-45. c) Frischmann, P. D.; MacLachlan, M. J. *Chem. Soc. Rev.* **2013**, *42*, 871-890. d) Han, Y.-F.; Li, H.; Jin, G.-X. *Chem. Commun.* **2010**, *46*, 6879-6890. e) Huang, C.-C.; Liu, J.-J.; Chen, Y.; Lin, M.-J. *Chem. Commun.* **2013**, *49*, 11512-11514.

[10] a) Garon, C. N.; Daigle, M.; Levesque, I.; Dufour, P.; Iden, H.; Tessier, C.; Maris, T.; Morin, J.-F.; Fontaine, F.-G. *Inorg. Chem.* **2012**, *51*, 10384−10393. b) Garon, C. N.; Gorelsky, S. I.; Sigouin, O.; Woo, T. K.; Fontaine, F.-G. *Inorg. Chem.* **2009**, *48*, 1699−1710. c) Sigouin, O.; Garon, C. N.; Delaunais, G.; Yin, X.; Woo, T. K.; Decken, A.; Fontaine, F.-G. *Angew. Chem., Int. Ed.* **2007**, *46*, 4979−4982.

[11] a) Iden, H.; Morin, J.-F.; Fontaine, F.-G. *Inorg. Chim. Acta* **2014**, *422*, 235-242. b) Iden, H.; Bi, W.; Morin, J.-F.; Fontaine, F.-G. *Inorg. Chem.* **2014**, *53*, 2883-2891.

[12] a) Zhou, Y.-K.; Chen, H.-M. *Polyhedron* **1990**, *9*, 2689−2691. b) Zhang, R.-F.; Li, C.-P.; Wang, Q.-F.; Ma, C.-L. *J. Coord. Chem.* **2010**, *63*, 2105−2112. c) Li, J.; Gao, Z.; Han, L.; Gao, L.; Zhang, C.; Tikkanen, W. *J. Organomet. Chem.* **2009**, *694*, 3444−3451.

[13] a) Kuate, A. C. T.; Pinkert, L.; Freytag, M.; Jones, P. G.; Tamm, M. *Z. Anorg. Allg. Chem.* **2013**, *639*, 2386-2389. b) Helmstedt, U.; Lebedkin, S.; Höcher, T.; Blaurock, S.; Hey-Hawkins, E. *Inorg. Chem.* **2008**, *47*, 5815-5820. c) Helmstedt, U; Lönnecke, P.; Reinhold, J.; Hey-Hawkins, E. *Eur. J. Inorg. Chem.* **2006**, *23*, 4922-4930. d) Pellny, P.-M.; Burlakov, V. V.; Baumann, W.; Spannenberg, A.; Rosenthal, U. *Z. Anorg. Allg. Chem.* **1999**, *625*, 910-918. e) Shah, S. A. A.; Dorn, H.; Gindl, J.; Noltemeyer, M.; Schmidt, H.-G.; Roesky, H. W. *J. Organomet. Chem.* **1998**, *550*, 1-6. f) Howard, W. A.; Trnka, T.; Waters, M.; Parkin, G. *J. Organomet. Chem.* **1997**, *528*, 95-121.

[14] a) Burlakov, V. V.; Arndt, P.; Baumann, W.; Spannenberg, A.; Rosenthal, U. *Organometallics* **2006**, *25*, 1317-1320. b) Burlakov, V. V.; Arndt, P.; Baumann, W.; Spannenberg, A.; Rosenthal, U. *Organometallics* **2004**, *23*, 4160-4165. c) Pellny, P.-M.; Kirchbauer, F. G.; Burlakov, V. V.; Baumann, W.; Spannenberg, A.; Rosenthal, U. *J. Am. Chem. Soc.* **1999**, *121*, 8313-8323. d) Yasuda, H.; Okamoto, T.; Matsuoka, Y.; Nakamura, A.; Kai, Y.; Kanehisa, N.; Kasai, N. *Organometallics* **1989**, *8*, 1139-1152.

[15] Li, J.; Gao, Z.; Han, L.; Gao, L.; Zhang, C.; Tikkanen, W. *J. Organomet. Chem.* **2009**, *694*, 3444-3451.

[16] Blenkers, J.; Hessen, B.; van Bolhuis, F.; Wagner, A. J.; Teuben, J. H. *Organometallics* **1987**, *6*, 459-469.

[17] Rogers, R. D.; Benning, M. M.; Kurihara, L. K.; Moriarty, K. J.; Rausch, M. D. *J. Organomet. Chem.* **1985**, *293*, 51-60.

[18] Jeffrey, G. A., *An introduction to hydrogen bonding*. Oxford University Press: Oxford, 1997.

[19] Chai, J.-D. ; Head-Gordon M. *Phys. Chem. Chem. Phys.* **2008**, *10*, 6615-20.

[20] (a) Francl, M. M.; Pietro, W. J.; Hehre, W. J.; Binkley, J. S.; Gordon, M. S.; Defrees, D. J.; Pople, J. A. *J. Chem. Phys.* **1982**, *77*, 3654-3665. (b) Hehre, W. J.; Ditchfield, R.; Pople, J. A. *J. Chem. Phys.***1972**, *56*, 2257-2261.

[21] Andrae, D.; Heussermann, U.; Dolg, M.; Stoll, H.; Preuss, H. *Theor. Chim. Acta.* **1990,** *77*, 123–141.

[22] Bai, G.; Roesky, H. W.; Li, J.; Labahn, T.; Cimpoesu, F.; Magull, J. *Organometallics* **2003**, *22*, 3034-3038.

[23] a) Wolczanski, P. T.; Bercaw, J. E. *Organometallics* **1982**, *1*, 793. (b) Manriquez, J. M.; Mcalister, D. R.; Rosenberg, E.; Shiller, A. M.; Williamson, K. L.; Chan, S. I.; Bercaw, J. E. *J. Am. Chem. Soc.* **1978**, *100*, 3078.

[24] *APEX2*; Bruker AXS Inc.: Madison, WI, 2007.

[25] *SAINT*; Bruker AXS Inc.: Madison, WI, 2007.

[26] Sheldrick, G. M. *SADABS*; Bruker AXS Inc.: Madison, WI, 2007.

[27] Sheldrick, G. M. *Acta Cryst.* **2008**, *A64*, 112-122.

[28] Spek, A. L. Acta Cryst. **2009**, *D65*, 148-155.

[29] Gaussian 09, Revision D.01, Frisch, M. J.; Trucks, G. W.; Schlegel, H. B.; Scuseria, G. E.; Robb, M. A.; Cheeseman, J. R.; Scalmani, G.; Barone, V.; Mennucci, B.; Petersson, G. *et al*., **2009**